# Menadione reduces *CDC25B* expression and promotes tumor shrinkage in gastric cancer

Amanda Braga Bona (iD), Danielle Queiroz Calcagno, Helem Ferreira Ribeiro, José Augusto Pereira Carneiro Muniz, Giovanny Rebouças Pinto, Carlos Alberto Machado Rocha, Antonio Carlos Cunha Lacreta Junior, Paulo Pimentel de Assumpção, Juan Antonio Rey Herranz and Rommel Rodriguez Burbano

## Abstract

**Background:** Gastric cancer is one of the most incident types of cancer worldwide and presents high mortality rates and poor prognosis. *MYC* oncogene overexpression is a key event in gastric carcinogenesis and it is known that its protein positively regulates CDC25B expression which, in turn, plays an essential role in the cell division cycle progression. Menadione is a synthetic form of vitamin K that acts as a specific inhibitor of the CDC25 family of phosphatases.

**Methods:** To better understand the menadione mechanism of action in gastric cancer, we evaluated its molecular and cellular effects in cell lines and in *Sapajus apella*, nonhuman primates from the new world which had gastric carcinogenesis induced by N-Methyl-N-nitrosourea. We tested CDC25B expression by western blot and RT-qPCR. *In-vitro* assays include proliferation, migration, invasion and flow cytometry to analyze cell cycle arrest. In *in-vivo* experiments, in addition to the expression analyses, we followed the preneoplastic lesions and the tumor progression by ultrasonography, endoscopy, biopsies, histopathology and immunohistochemistry.

**Results:** Our tests demonstrated menadione reducing CDC25B expression *in vivo* and *in vitro*. It was able to reduce migration, invasion and proliferation rates, and induce cell cycle arrest in gastric cancer cell lines. Moreover, our *in-vivo* experiments demonstrated menadione inhibiting tumor development and progression.

**Conclusions:** We suggest this compound may be an important ally of chemotherapeutics in the treatment of gastric cancer. In addition, CDC25B has proven to be an effective target for investigation and development of new therapeutic strategies for this malignancy.

*Keywords:* CDC25B, gastric cancer, menadione, *MYC*, *Sapajus apella*

Correspondence to:
**Amanda Braga Bona**
Oncology Research Laboratory, Ophir Loyola Hospital, Governador Magalhães Barata Avenue, 992 Belém, PA, 66063-240, Brazil Biological Sciences Institute, Federal University of Pará, Belém, Brazil
**amandabbona@gmail.com**

**Danielle Queiroz Calcagno**
**Paulo Pimentel de Assumpção**
Oncology Research Nucleus, University Hospital João de Barros Barreto, Federal University of Pará, Belém, Brazil

**Helem Ferreira Ribeiro**
Center of Biological and Health Sciences, Department of Biomedicine, University of Amazon, Belém, Brazil

**José Augusto Pereira Carneiro Muniz**
National Center of Primates, Health Ministry, Ananindeua, Brazil

**Giovanny Rebouças Pinto**
Department of Biomedicine, Federal University of Piauí, Parnaíba, Brazil

**Carlos Alberto Machado Rocha**
Federal Institute of Education, Science and Technology

**Antonio Carlos Cunha Lacreta Junior**
Department of Veterinary Medicine, Federal University of Lavras, Lavras, Brazil

**Juan Antonio Rey Herranz**
Molecular Oncogenetics Laboratory, Research Unit, Hospital Universitario La Paz, Madrid, Spain

**Rommel Rodriguez Burbano**
Laboratory of Molecular Biology, Ophir Loyola Hospital, Belém, Brazil

## Introduction

Gastric cancer (GC) is one of the most commonly occurring types of cancers worldwide[1] and presents high mortality rates and poor prognosis.[2] Despite this, gastric carcinogenesis remains far from being fully understood. To obtain a better understanding of this process, our research group developed an experimental model in nonhuman primates, *Sapajus apella* (*S. apella*), using N-Methyl-N-nitrosourea (MNU). In this model, the amplification and overexpression of *MYC* gene were commonly observed.[3] MYC is a critical transcriptional factor associated to several cellular activities, including cell cycle progression.[4] Moreover, MYC has been demonstrated as a key element in gastric carcinogenesis and it is frequently observed to be deregulated in stomach tumors.[5–8] According to Da Costa and colleagues,[3] MYC-regulated genes also undergo changes by MNU-induced carcinogenesis progress. Therefore,

identifying MYC target genes is a crucial step for knowledge of gastric tumorigenesis and the development of new anticancer therapies.

Cell division cycle 25 (CDC25), a group of three (CDC25A; CDC25B; CDC25C) highly conserved enzymes that play essential roles in cell cycle progression,[9] is one of the MYC protein targets.[10] In a previous study, the silencing of the *MYC* gene in GC cell lines, followed by next-generation sequencing, allowed the detection of more than 5000 DEGs (differentially expressed genes) regulated by this transcription factor. Of this ratio, the *CDC25B* gene was found to be in the 10 most prevalent and differentiated genes.[11] In addition, analyses in clinical samples revealed that the increase in *CDC25B* expression is associated with the early onset of gastric tumors.[12]

The *CDC25B* gene encodes a dual-specificity phosphatase that induces the cell division by activating Cdk1–Cyclin B complexes, which in turn are responsible for the G2/M transition during cell cycle progression.[13,14] The phosphatase CDC25B plays the abovementioned role by the dephosphorylation of the adjacent phosphothreonine and phosphotyrosine residues, pThr14 and pTyr15, on the cyclin-dependent kinases 1 (CDK1) subunit; therefore, it is fundamentally required for cell entry into mitosis.[13,14] In addition, the constitutive CDK activation causes an overphosphorylation of proteins that promote cell cycle progression,[13] thus increased activity of CDC25B may be closely related to tumor development and progression. This phosphatase has been described as overexpressed in many different types of cancer, including GC.[15–17] Herewith, CDC25B inhibitors, such as menadione (MD), might be a useful therapy strategy against these tumors.

MD is a synthetic analog of vitamin K and acts as a specific inhibitor of CDC25 phosphatases by interacting with the active site of the protein and forming a covalent bond, thus preventing the enzyme performing its function.[18] Some studies have described MD inhibiting cell proliferation and inducing apoptosis in different types of cancer.[19–21] A recent study showed that *CDC25C* expression decreases in an MD dose-dependent manner in GC cells, suggesting this compound inhibits tumor cells' growth by reducing *CDC25C* expression.[22] To our knowledge, this is the first study associating the silencing of the *CDC25B* gene and the use of MD in GC. We aimed to analyze MD potential, *in vitro* and *in vivo*, as an antitumoral agent through the inhibition of *CDC25B* expression, evaluating its ability to prevent tumor development and tumor progression.

## Materials and methods

### Cell lines and culture
In the present study we used three GC cell lines established by our research group, derived from patients from the state of Pará, Brazil. Cell line AGP01 was established from the ascitic fluid of an individual with metastatic intestinal-type GC, ACP02 from diffuse-type GC, and ACP03 from intestinal-type GC.[23] All cell lines present *MYC* amplification and chromosome 8 trisomy, where *MYC* is located.[23,24] It has also been demonstrated that all three cell lines show increased mRNA and protein expression of MYC and CDC25B.[12] MNP01 (Normal Gastric Mucosa Cell Line 01), cell culture of non-neoplastic gastric mucosa cells pooled from 10 patients without GC, which was also established by our research group, was used to evaluate the normal *CDC25B* mRNA and protein expression.

Cell lines were cultivated in Dulbecco's modified Eagle's medium (DMEM; Gibco/ThermoFisher, Waltham, MA, USA) and supplemented with 10% fetal bovine serum (FBS; Gibco/ThermoFisher, USA) and antibiotics (100 µg/ml streptomycin; 100 U/ml penicillin; 0.25 µg/ml amphotericin B). All cell lines were maintained in a humidified atmosphere at 37°C containing 5% $CO_2$.

### Cell viability
*Colorimetric MTT assay.* Tetrazolium salt was diluted in phosphate-buffered saline (PBS) to a concentration of 5 mg/ml. Cells were cultured in 6 cm² plates at a concentration of $3 \times 10^5$. Each well received 50 µl of tetrazolium salt and the plate was then incubated for 3 h under normal culture conditions. MD was tested in three different concentrations (0.5 µM; 1.0 µM; 25 µM), while the corresponding nontreated cell line was used as the negative control. For colorimetric analysis, MTT formazan crystals were solubilized in isopropanol and quantified by spectrophotometry at a wavelength of 570 nm. The viability percentage of all test samples was calculated using the mean absorbance of each sample, considering

the negative absorbance mean of negative control as 100%.[25] All tests were performed three times and in triplicate.

*Trypan blue dye exclusion assay.* Cells at 80–90% confluence were harvested and plated on a six-well plate at a $2 \times 10^5$ concentration of cells per well in a final volume of 2 ml of complete DMEM media. MD was tested in three different concentrations ($0.5 \mu M$; $1.0 \mu M$; $25 \mu M$), while the corresponding nontreated cell line was used as the negative control. After treatment, cells were incubated for 48 h at 37°C in a 5% $CO_2$ incubator and then counted using a standard hemocytometer-based cell-counting method. Tests were performed three times and in triplicate.

*Small interfering RNA (siRNA) transfection and menadione treatment.* An amount of $3 \times 10^5$ cells of each cell line were seeded into 6 cm$^2$ plates before transfection and MD treatment. Cells were cultured for 24 h until cell density was approximately 50%. For *CDC25B* silencing by siRNA, all the GC cell lines were transfected using Silencer Select siRNA specific for *CDC25B* (s2753; #4390824; Ambion, Foster City, CA, USA). For *CDC25B* inhibition by MD evaluation, all three cell lines were treated with MD at a concentration of 25 $\mu M$ (Sigma-Aldrich, St. Louis, MO, USA) for 48 h and the results were compared with siRNA silencing values. For each cell line, the control was the cell line itself before the MD treatment or siRNA transfection. All siRNA and MD experiments were performed three times.

## Cell proliferation by direct counting

Briefly, AGP01, ACP02 and ACP03 cells were harvested after 24, 48 and 72 h of siRNA transfection and MD treatment, and directly counted in Neubauer chambers. The total number of cells estimated was used to determine cell proliferation. All three times, the experiments were carried in triplicate.

## Migration and invasion analysis

Migration and invasion experiments were carried out in a modified Boyden chamber with 8 $\mu m$ pore filter inserts for 12-well plates (BD Biosciences, San Jose, CA, USA). Particularly in invasion experiments, filters were coated with 10 $\mu l$ of Matrigel (10–13 mg/ml) (BD Biosciences, San Jose, CA, USA) and stored overnight. For both experiments, after siRNA transfection and MD treatment, $2 \times 10^5$ cells of each cell line were plated into the upper chamber in 1 ml of DMEM without FBS. The lower chamber was filled with 1.5 ml of DMEM with FBS and cells were incubated at 37°C in a 5% $CO_2$ incubator for 18 h and 48 h for migration and invasion assays, respectively. Then, cells were fixed with 4% paraformaldehyde and post-fixed with 0.2% crystal violet in 20% methanol. Cells on the upper side of the filter, including those in the Matrigel, were removed with a cotton swab. Invading cells (on the lower side of the filter) were photographed and counted. All experiments were carried in triplicate.

## Cell cycle analysis by flow cytometry

For the cell cycle analysis, siRNA transfection and MD treatment were carried for 72 h. Cells were treated with 10 $\mu M$ BrdU (Sigma-Aldrich, USA) for 60 min, trypsinized and then fixed in 80% ethanol at −20°C overnight. Then, the cell pellet was treated with 2 M HCl/0.5% Triton X-100 (Sigma-Aldrich, USA) for 30 min at room temperature, neutralized with 0.1 M $Na_2B_4O_7$, and stained with FITC-anti BrdU antibodies (Sigma-Aldrich, USA). Posteriorly, the cells were centrifuged at 1000 rpm for 5–7 min and 400 $\mu l$ of propidium iodide (PI)-RNase solution (38 mM $Na_3C6H_5O_7 + 69 \mu M$ PI + 1 $\mu l$ of 10 mg/ml RNase A) (ThermoFisher, USA) was added to the pellet and resuspended well. Samples were incubated in the dark for 30 min at 37°C before analysis by BD FACSCanto™ II (BD Biosciences, USA) flow cytometer. All cell lines were analyzed three times. The forward light scatter (FSC) of nonfixed cells was used as a relative measure of cell size.

## Animal experimentation: Sapajus apella

*Experimental design.* To define the sample number of the experimental design we relied on the concepts of *replacement, reduction,* and *refinement* (3Rs) established by Russell and Burch[26] in the book *The Principles of Humane Experimental Technique,* which remains a reference for studies using animal models.[27]

In total, taking into account the concepts of Russell and Burch,[26] the needs of the study and the maximum number of animals allowed by the ethics committee, we used 20 adult male primates (around 6 years old), weighing between 2.6 and

3.5 kg. The animals were obtained and allocated in the Centro Nacional de Primatas (National Primates Center), in the state of Pará, Brazil, where they were fed with a healthy and balanced diet, not enriched with sodium chloride, and weighed daily. Each animal was identified with a microchip, and throughout the entire treatment they were inspected daily, and their clinical symptoms were recorded. Additionally, blood samples of all animals were collected for hematological and biochemical analysis according to Da Costa and colleagues[3] All animals underwent veterinary examinations before the start of the experiments and were considered healthy for the first blood collection, endoscopy, and ultrasonography. We followed, according to the Weatherall report 'The use of non-human primates in research', all the necessary recommendations to maintain the animals' welfare and alleviate their suffering. This study was approved by the Ethics Committee of Federal University Pará (PARECER MED-002-13).

*In-vivo* experiments were performed in two different models.

*Model 1: cell lines inoculation.* 12 primates were randomly split into three groups of four animals:

- Cell line group (CL): four *S. apella* inoculated with GC cell line and treated with saline solution injections instead of MD for 14 days.
- Cell line plus MD 1 group (CLMD1): four *S. apella* inoculated with GC cell line and then treated with MD at a concentration of 2.5 g/m² since day 5 of cell line inoculation in a total of 14 days.
- Cell line plus MD 2 group (CLMD2): four *S. apella* inoculated with GC cell line and treated with MD at a concentration of 2.5 g/m² concomitantly for 14 days.

*Model 2: MNU inoculation.* Eight primates were randomly split into two groups of four animals:

- MNU group: four *S. apella* treated with MNU for 960 days.
- MNU + MD group: four *S. apella* treated with MNU plus 2.5 g/m² of MD concomitantly for 960 days (since day 0).

*Cell line inoculation.* A cell line concentration of 10¹⁰ was inoculated in the animals percutaneously,

between the mucosal and submucosal layers of the antral region of the stomach, according to the protocol established by Da Costa and colleagues,[3] which determined ACP03 as the standard for the process of tumorigenesis in nonhuman primates. One week before the cell line inoculation, all primates were immunosuppressed by a single dose of 50 mg/kg of cyclophosphamide (Sigma-Aldrich, USA). Ultrasonography was used to visualize the stomach tissues during cell line inoculation.

*Menadione treatment.* For MD treatment the concentration of 2.5 g/m² was determined based on a therapeutic scheme used in human patients which was adapted for *S. apella*, taking into account the weight of the animal.[28,29] Doses were calculated at the time of injection, according to the animal's weight. MD was injected by slow infusion in the right or left femoral vein of primates, alternating when needed, in a single dose daily. Veins of arms or neck can also be used if necessary to avoid pain for the animals. Experiments were performed with commercial MD acquired on the Sigma-Aldrich website (Sigma-Aldrich, USA). Water was given *ad libitum* during MD treatment.

*MNU treatment.* MNU treatment followed precisely the protocol established by Da Costa and colleagues[3] All animals received fresh oral doses of MNU (N1517; Sigma-Aldrich, USA) daily for 960 days at a dosage of 16 mg/kg body weight. The animals also received drinking water containing MNU in light-shielded bottles daily. Water was restricted during MNU treatment.

*MNU and MNU + MD groups follow up.* Gastric mucosa alterations and tumor growth were followed by endoscopy examination and ultrasonography. The animals were submitted to endoscopy before, during, and after the period of treatments and biopsy samples were collected from healthy and non-normal gastric mucosa tissue (e.g. nonatrophic gastritis; atrophic gastritis; metaplasia; neoplasia). Biopsies were collected on days 0, 90, 120, 300 and 960 of the treatment with MNU and MNU + MD, and a pachymeter was used to measure the tumor biopsies. For histological and immunohistochemical analysis, part of each *S. apella* gastric mucosa biopsy sample was embedded in paraffin, cut in 5 mm sections, and stained by hematoxylin and eosin. All samples were histologically classified according to Lauren.[30]

*Menadione treatment after tumor development.* It was necessary to remove four primates from the second model of the study to avoid their death, leaving only two in each group. These animals were presenting symptoms of high toxicity due to treatment with MNU. One of the two remaining *S. apella* from the MNU group was treated with MD in three cycles of two days (one dose daily), with a cycle every 21 days from day 990 (30 days of rest after MNU-alone treatment). This protocol was adapted from Tetef and colleagues[28,29] The animal had 28 days of rest after the three MD cycles. On day 1060, both the treated and non-treated animals were submitted to surgical removal of the tumor, and the tumor size was evaluated and compared between the two animals. CDC25B protein and mRNA expression were tested by western blot and real-time reverse transcription quantitative PCR (RT-qPCR), respectively, and compared between primates.

### mRNA and protein expression analysis

In cell lines, both assays were performed before and after siRNA silencing and MD treatment. The MNP01 Cell Line was used as a negative control. In the second model of nonhuman primates, the tests were performed on days 0, 90, 120, 300 and 960 (day 0 was used as a calibrator). In the first model, we could not obtain tumor samples.

### DNA/RNA/protein extraction and purification

In cell line assays, the total RNA and proteins were extracted after 48h of siRNA transfection and MD treatment with TRIzol reagent. For the *S. apella* experiments, we used the AllPrep DNA/RNA/Protein Kit (Qiagen, Hilden, Germany) which works perfectly for these primates.[3] The total protein, mRNA and DNA were simultaneously isolated from healthy and non-normal gastric tissue samples obtained by endoscopy and surgical resection according to the manufacturer's instructions. The protein pellet was dissolved in a buffer containing 7 M urea, 2 M thiourea, 4% CHAPS, 50 mM DTT, 1% Protease Inhibitor Cocktail (Sigma-Aldrich, USA), and 0.5% each of Phosphatase Inhibitor Cocktail 1 and 2 (Sigma-Aldrich, USA), following the protocol of Leal and colleagues[31] To determine the protein concentrations, we used the method of Bradford (Sigma-Aldrich, USA). The RNA quality was tested by 1% agarose gels and the concentration was

determined using NanoDrop spectrophotometer (Kisker Biotech, Steinfurt Germany). Samples were stored at −80°C until use.

*mRNA expression.* Complementary DNA was manufactured using the Reverse Transcription System according to the manufacturer's protocol (A3500; Promega, Madison, WI, USA), then amplified by RT-qPCR using TaqMan probes purchased as Assays-on-Demand Products for Gene Expression (Life Technologies, Carlsbad, CA, USA) and a 7500 Fast Real-Time PCR instrument (Life Technologies, USA). The *GAPDH* gene was selected as an internal control.[3] All RT-qPCRs were performed in triplicate for the target gene (*CDC25B*: Hs00244740_m1) and the internal control (*GAPDH*: NM_002046.3).

The relative quantification (RQ) of gene expression was calculated according to Livak and Schmittgen.[32] In tissue sample analyses, the corresponding control sample was designated as a calibrator from each tumor. In the cell line analysis, the siRNA control-transfected cells were used as a calibrator. The gene expression in the MNP01 was also designated as a calibrator from all GC cell lines.

*Western blotting.* Western blot assay was performed as previously described by our research group.[31] A total of 25 μg of the reduced protein from each sample was separated by 12.5% homogeneous sodium dodecyl sulfate-polyacrylamide gel electrophoresis (SDS-PAGE) and then transferred to a polyvinylidene fluoride (PVDF) membrane (Hybond-P; GE Healthcare, Chicago, IL, USA). To block the PVDF membrane we used PBS containing 0.1% Tween 20 and 5% low-fat milk, and then the membrane was incubated overnight at 4°C, with the primary antibody of the target genes: anti-*CDC25B* (dilution 1:1000; PA5-14100; Life Technologies, USA), and anti-ACTB (dilution 1:250; Ac-15; Life Technologies, USA) used as a loading reference control. For cell cycle analyses, we used rabbit polyclonal antibody against Phospho-CDK1 (Tyr15) (dilution 1:500; PA5-85508, Invitrogen, USA) and mouse monoclonal antibody against Cyclin B1 (dilution 1–3 μg/ml; MA5-13128; Invitrogen USA), and anti-ACTB as a loading reference control. After extensive washing, a peroxidase-conjugated secondary antibody (Life Technologies, USA) was added for 1 h at room temperature.

Immunoreactive bands were visualized using the western blotting Luminol reagent (Life Technologies, USA), and images were acquired using an ImageQuant 350 digital image system (GE Healthcare, USA).

### Immunohistochemical analysis

Primates' gastric tissue sample sections were deparaffinized in xylene and then rehydrated in a graded series of ethanol. After heat-induced epitope retrieval, we incubated the tissue sections with primary mouse monoclonal antibody against CDC25B (dilution 1:10; PA5- 14100; Life Technologies, USA). The universal peroxidase-conjugated secondary antibody kit (LSAB System; DakoCytomation, Glostrup, Denmark) was used for detection. We used 3,3'-diaminobenzidine/$H_2O_2$ (DakoCytomation, Denmark) as the chromogen, and hematoxylin was used as the counterstain. The expression of *CDC25B* in GC cells was evaluated using light microscopy with a semiquantitative scale: 0 pt − no reaction, 1 pt − weak reaction, 2 pts − moderate reaction and 3 pts − intense reaction. The classification given to each tissue section was calculated according to the average of the counts made in five fields at 400× magnification, selected at random.[33]

### Statistical analysis

As all *in-vitro* experiments were repeated three times, the results are presented as mean ± standard deviation (SD). Statistical analyses were performed using GraphPad 8.0.1 statistical software (GraphPad Software, San Diego, CA, USA). For all *in-vitro* experiments, *p* values were calculated twice: grouped, using one-way analysis of variance (ANOVA); and separately, using paired Student's *t* test. *In-vivo* experiments were analyzed separately for each day using unpaired Student's *t* test. As at the end of MNU treatment only two primates were available for the study, only one animal was treated with MD for comparison with the nontreated animal; therefore it was not possible to perform statistical analyses. However, as the mRNA and protein expression numbers were very similar to the data obtained for cell lines analyses and MNU/MNU + MD group comparison, we assume the significance may follow the same pattern. *p* values < 0.05 were considered as statistically significant differences.

## Results

### Cell lines

To evaluate MD toxicity, we performed cell survival assays in all three GC cell lines and could not find significance in any of the tested concentrations, demonstrating that MD does not present cytotoxicity in the concentrations used to perform our experiments (Figure 1). On the other hand, a very significant decrease in proliferation, invasion and migration levels were observed after MD treatment, following the same pattern of gene silencing by interfering RNA (Figure 1).

In addition, the flow cytometry assay demonstrated that MD treatment induced cell cycle arrest in the G2/M phase (Figure 2). To confirm cell cycle arrest, we tested the expression of Cyclin B1 and p-CDK1 by western blot. It is well known that high levels of these proteins indicate cell cycle arrest at the G2/M phase. Our results demonstrated the overexpression of both proteins after MD treatment, which indicates the presence of the inactive Cyclin B–CDK1 complex, confirming cell cycle arrest (Figure 2).

Furthermore, western blot and RT-qPCR assays showed *CDC25B* expression levels significantly reduced after MD treatment in all three GC cell lines (Figure 3)

### Animal experiments

In the first model of animal experimentation, the primates of the CL group presented tumor lesions in the antral region of the stomach on the ninth day of ACP03 inoculation. Tumor volumes were similar in all animals and they were able to naturally eliminate tumors by day 14. However, in both CLMD1 and CLMD2 groups none of the primates had any type of tumor development.

In the second animal model, until day 300, *CDC25B* mRNA and protein expression levels were slightly lower in animals of the MNU + MD group compared to animals of the MNU group. However, at day 960 both expression levels were around 40% lower in the animals treated with MD (Figure 4). The animal of MNU group that was treated with MD after tumor development presented a considerable decrease in *CDC25B* mRNA and protein expression levels at the time of surgical tumor extraction when compared to day 990 and to the nontreated animal (Figure 4).
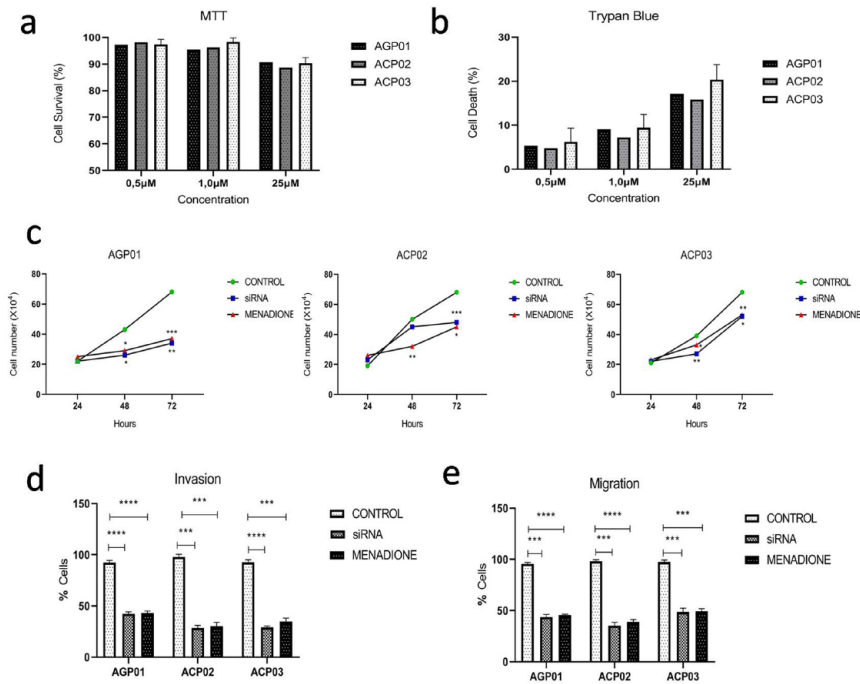
**Figure 1.** Menadione does not show cytotoxicity effects but can reduce invasion, migration and proliferation rates. (a) Percentage of cell viability analyzed by MTT for all three cell lines after MD treatment in different concentrations. Data were evaluated compared to the control group (respective nontreated cell lines). No significant differences were found between the treated and nontreated cells or the different drug concentrations. (b) Percentage of cell death analyzed by direct count with trypan blue. Data were evaluated compared to the control group (respective nontreated cell lines). No significant differences were found between the treated and nontreated cells or the different drug concentrations. (c) Menadione significantly reduced proliferation rates in all three cell lines. (d) Menadione significantly reduced invasion rates in all three cell lines. (e) Menadione significantly reduced migration rates in all three cell lines. The control groups are the respective nontreated cell line. Data were obtained from triplicate experiments and analyzed by one-way analysis of variance (ANOVA) and paired Student's *t* test.
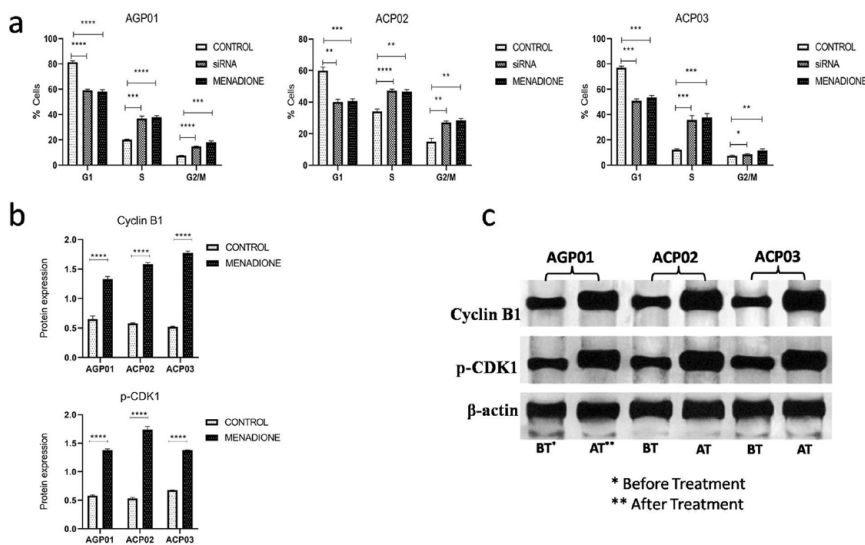$^*p < 0.05$, $^{**}p < 0.01$, $^{***}p < 0.001$, $^{****}p < 0.0001$.



**Figure 2.** Menadione induced cell cycle arrest at the G2/M phase. (a) Cell cycle analysis by flow cytometry showing a significant increase in the percentage of cells at G2/M phase after the treatment with menadione in all three GC cell lines. (b) Menadione high significantly increased protein expression of Cyclin B1 and p-CDK1, confirming its potential to arrest cell cycle progression at the G2/M phase. (c) Protein expression of Cyclin B1 and p-CDK1 demonstrated by western blot. The control groups are the respective nontreated cell line.
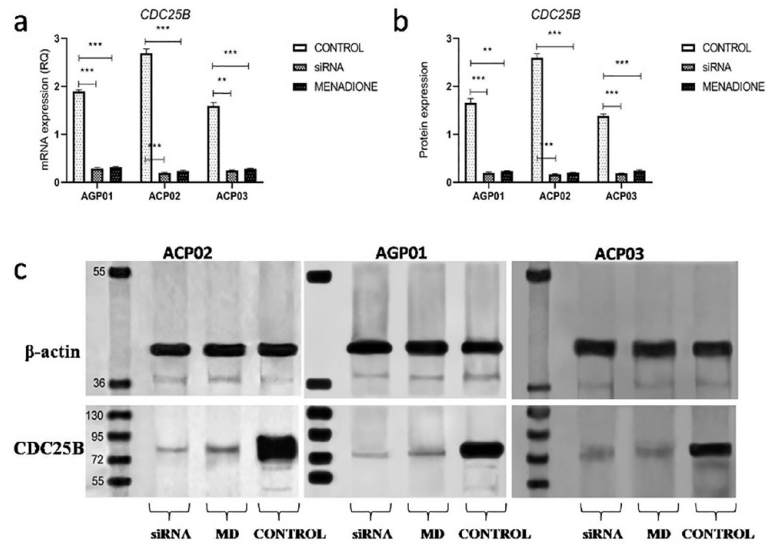
**Figure 3.** Menadione reduces *CDC25B* mRNA and protein expression in CG cell lines. (a) Comparison of MD and small interfering RNA effects on *CDC25B* mRNA expression in GC lines. (b) Comparison of MD and small interfering RNA effects on CDC25B protein expression in GC cell lines. (c) CDC25B protein expression in GC cell lines analyzed by western blot after MD treatment and siRNA transfection; equal amounts of whole-cell extracts were analyzed using the indicated antibodies. The control groups are the respective nontreated cell line. Data were analyzed by one-way analysis of variance (ANOVA) and paired Student's *t* test.
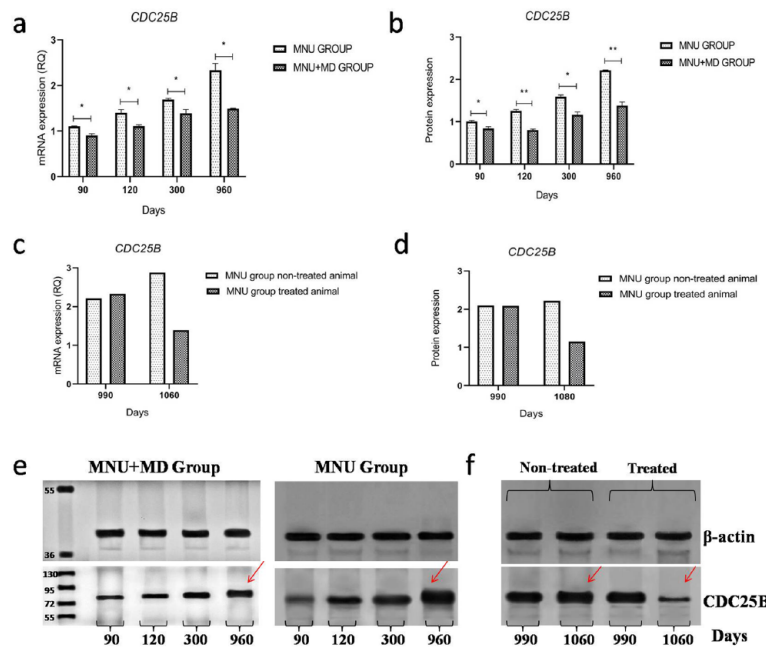$**p < 0.01$, $***p < 0.001$.



**Figure 4.** Menadione (MD) reduces *CDC25B* mRNA and protein expression in *S. apella* gastric tumor tissue and prevents gastric adenocarcinoma development. (a) Effects of the daily MNU + MD treatment on *CDC25B* mRNA expression during 960 days; (b) effects of the daily MNU + MD treatment on *CDC25B* protein expression during 960 days; (c) effects of MD treatment after MNU-induced carcinogenesis on *CDC25B* mRNA expression; (d) effects of MD treatment after MNU-induced carcinogenesis on *CDC25B* protein expression; (e) representative image of CDC25B protein expression analyzed by western blot of MNU + MD and MNU group animals throughout the 960 days of treatment. The red arrows indicate the difference of *CDC25B* expression between the two groups on the last day of treatment, when the animals of the MNU group developed gastric adenocarcinoma and animals of MNU + MD group stagnated in metaplasia. (f) Effects of MD on protein expression levels of one MNU group primate before and after MD treatment analyzed by western blot. The red arrows indicate the difference of *CDC25B* expression between the treated and nontreated animals in the day of tumor surgical removal. Data were analyzed by unpaired Student's *t* test.
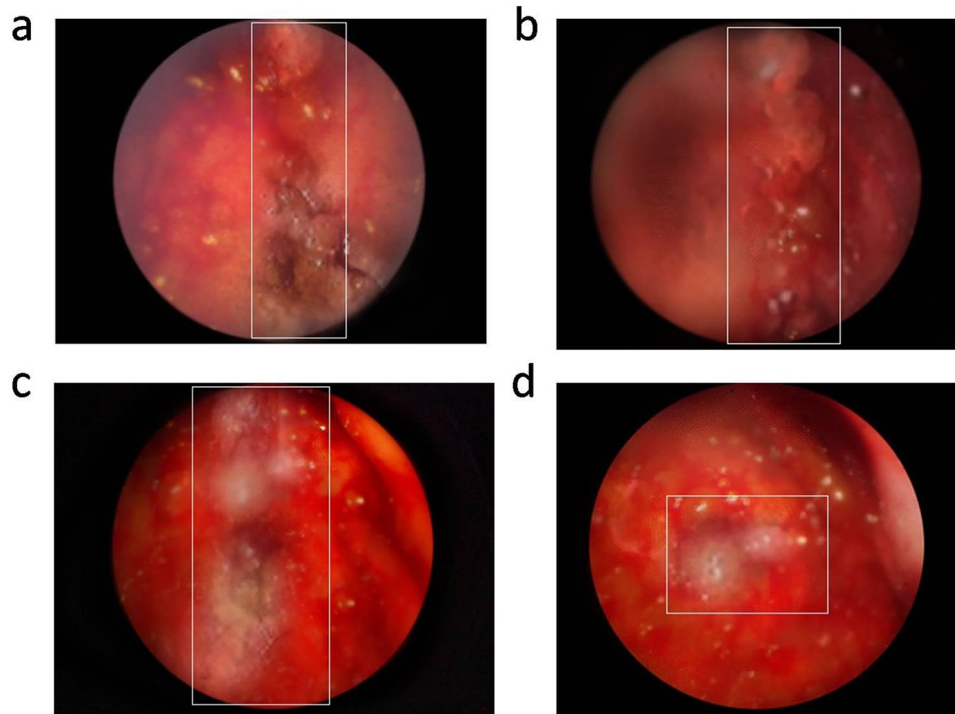MNU, Methyl-N-nitrosourea; $*p < 0.05$, $**p < 0.01$.

**Figure 5.** Menadione (MD) promoted tumor shrinkage. Gastric tissue images made by upper digestive endoscopy of the Methyl-N-nitrosourea (MNU) group primates. (a) and (b) Images of the same animal on different days. (a) Adenocarcinoma gastric lesion of the primate treated with MNU alone on day 990. This animal did not undergo MD treatment. (b) Adenocarcinoma gastric lesion of the primate with no MD treatment on day 1060, before surgical resection. When comparing the two images, we can observe a considerable reduction of the local inflammation due to the suspension of the MNU treatment, but there was no visual reduction of tumor size. (c) and (d) Images of the same animal on different days. (c) Adenocarcinoma gastric lesion of the primate treated with MNU alone on day 990. This animal underwent MD treatment. (d) Adenocarcinoma gastric lesion after the three MD treatment cycles, on day 1060, before surgical resection. Between these two images, it is possible to observe, in addition to the reduction of local inflammation, a substantial shrinkage of the tumor lesion in the primate treated with MD.

It may explain the reasonable shrinkage of the tumor observed in this primate after MD treatment (Figure 5).

The carcinogenic process in the animals of the MNU group followed the same pattern previously described by Da Costa and colleagues:[3] nonatrophic gastritis (day 90); atrophic gastritis (day 120); metaplasia (day 300); and intestinal-type adenocarcinoma in the antral region of the stomach (day 960) (Figure 6). Not surprisingly, on day 300, the animals of the MNU + MD group presented the same carcinogenic evolution as the animals treated with MNU alone, but, differently to the MNU group, the primates treated with MD had no evolution to gastric adenocarcinoma, and the lesion stagnated in metaplasia (Figure 4).

Furthermore, in the immunohistochemistry assays, performed using the primates' samples obtained by biopsies, we noticed that in the normal gastric tissue the immunoreactivity of *CDC25B* is very low (0 points in the semiquantitative analysis), but it gradually increases, from 0 to 3 points, with the evolution of the preneoplastic lesions (Figure 6(a.1–e.1)). The highest *CDC25B* immunoreactivity (3 points on the semiquantitative scale) was observed in the malignant tissue samples (Figure 6(e.1)); however, when analyzing the same animal after being treated with three cycles of MD, it showed a significant decrease in the immunoreactivity of *CDC25B* (2 points on the semiquantitative scale) (Figure 6(f.1)).

In atrophic gastritis (Figure 6(c.1)), metaplasia (Figure 6(d.1)) and intestinal-type gastric adenocarcinoma (Figure 6(e.1)), the protein was found mainly located in nuclei, and weak expression in cytoplasm was observed in some cells. Moreover, in intestinal-type gastric adenocarcinoma, after the MD treatment, the protein was found located in nuclei, but not in cytoplasm (Figure 6(f.1))
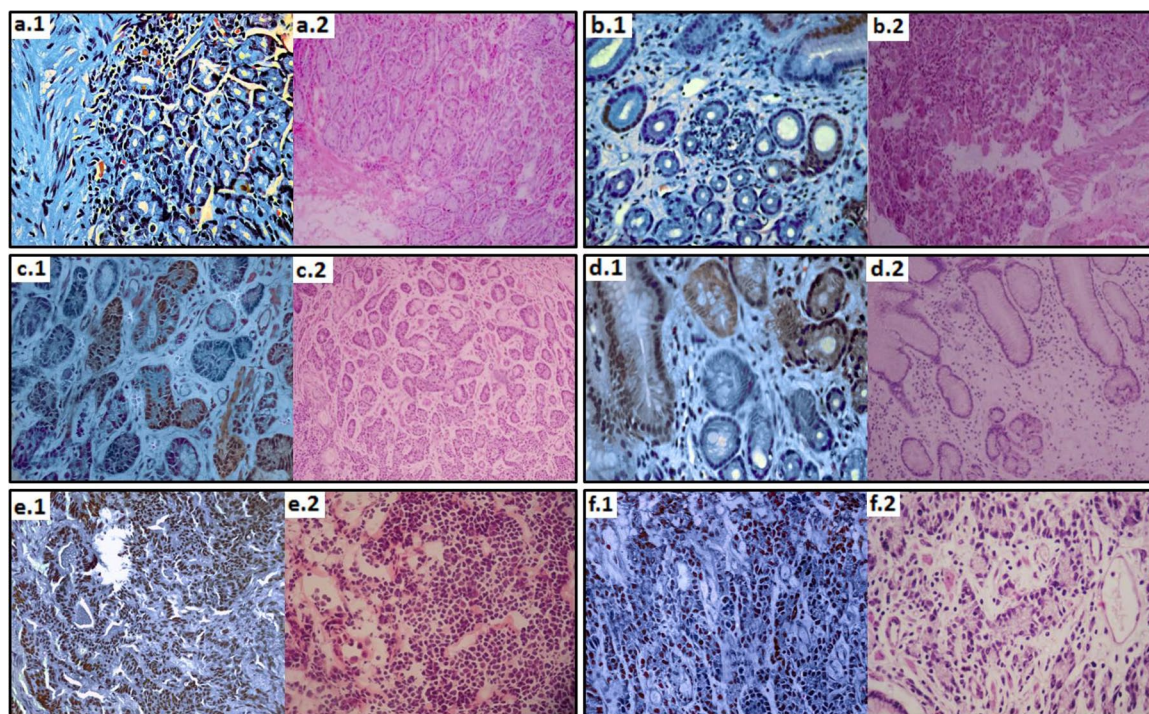
**Figure 6.** The evolution of gastric carcinogenesis in *Sapajus apella* showing *CDC25B* immunoreactivity.
(a.1) Non-neoplastic gastric mucosa, at 400× microscopic magnification, collected at day 0, showing very low immunoreactivity of *CDC25B*, that is, 0 points on semiquantitative immunohistochemical assessment scale; (a.2) non-neoplastic gastric mucosa, at 100× microscopic magnification, collected at day 0, stained with hematoxylin–eosin; (b.1) gastritis preneoplastic lesion, at 400× microscopic magnification, collected at day 90 of an Methyl-N-nitrosourea (MNU) group animal, showing a slight increase of *CDC25B* immunoreaction, but still considered as 0 points in the semiquantitative immunohistochemical evaluation scale; (b.2) gastritis, at 100× microscopic magnification, collected at day 90 of an MNU group animal, stained with hematoxylin–eosin; (c.1) atrophic gastritis preneoplastic lesion, at 400× microscopic magnification, collected at day 120 of an MNU group animal, showing a higher increase of *CDC25B* immunoreaction, which was considered as 1 point on the semiquantitative immunohistochemical evaluation scale; (c.2) atrophic gastritis, at 100× microscopic magnification, collected at day 120 of an MNU group animal, stained with hematoxylin–eosin; (d.1) metaplasia preneoplastic lesion, collected at day 300 of an MNU group animal, at 400× microscopic magnification, showing a considerable increase of *CDC25B* immunoreaction, corresponding to 2 points on the semiquantitative immunohistochemical analysis scale; (d.2) metaplasia, at 100× microscopic magnification, collected at day 300 of an MNU group animal, stained with hematoxylin–eosin; (e.1) intestinal-type gastric adenocarcinoma, at 400× microscopic magnification, collected at day 960 of an MNU group animal, showing a very increased immunoreactivity of *CDC25B*, corresponding to 3 points on the semiquantitative immunohistochemical analysis scale; (e.2) intestinal-type gastric adenocarcinoma, at 400× microscopic magnification, collected at day 960 of an MNU group animal, stained with hematoxylin–eosin; (f.1) intestinal-type gastric adenocarcinoma after menadione (MD) treatment, at 400× microscopic magnification, collected at day 1060, showing a reasonable decrease of *CDC25B* immunoreaction, corresponding to 2 points on the semiquantitative immunohistochemical analysis scale; (f.2) intestinal-type gastric adenocarcinoma after MD treatment, at 400× microscopic magnification, collected at day 1060, stained with hematoxylin–eosin. In c.1, d.1 and e.1, the protein was found mainly located in nuclei, with weak expression in cytoplasm observed in some cells. But in f.1, the protein was found located in the nuclei only, not in cytoplasm.

## Discussion

Studies have demonstrated that, in addition to being directly related to tumor progression in GC, *MYC* overexpression promotes proliferation, invasion and migration in tumor cells.[5,34] We suggest that *MYC* plays these roles by inducing CDC25B expression; therefore, inhibiting this phosphatase may block the consequences of *MYC* amplification on gastric carcinogenesis and on tumor cells. This hypothesis explains our *in-vitro* tests results, which demonstrated a highly significant decrease of cell proliferation, invasion and migration rates in all three GC cell lines after MD treatment tests. Our data corroborate the results of Leal and colleagues,[24] which had already demonstrated *CDC25B* silencing reducing all three rates in GC cell lines regardless of *MYC* expression levels. As Lee and colleagues[22] demonstrated while studying *CDC25C*, our cell cycle analyses by flow cytometry and western blot showed that the silencing of the *CDC25B* gene induced cell cycle arrest in the G2/M transition phase, which justifies the reduced values of cell proliferation.

Moreover, the reduced levels of *CDC25B* mRNA and protein can explain the lower proportions of invasion, migration and proliferation. We believe this fact is due to the MD mechanism of action that inactivates *CDC25B*, reduces the active protein expression and induces cell cycle arrest. Consequently, the lower cellular activity influences the cell division signaling process and negatively regulates the mRNA expression of *CDC25B*. The decline in expression levels combined with the other *in-vitro* data reinforces our hypothesis that it is due to *CDC25B* overexpression, induced by MYC protein, that gastric tumor cells acquire their most aggressive characteristics.

In the first model of animal experimentation, using cell line injections, we observed a potential antitumor action of MD. The primates that received MD concomitantly with cell lines (CLMD1 and CLMD2 groups) did not present tumor development, and it is likely that MD had directly acted on the cell line. Therefore, MD would act to block the cell cycle progression, decreasing the infiltrative capacity of cells and preventing their adhesion in the primates' normal gastric mucosa.

Our results from the second animal model experiments showed that MD was able to reduce *CDC25B* mRNA and protein expression levels in the primates' gastric tissue. Furthermore, the animals treated with MD concomitantly with MNU, differently to the MNU group animals, did not develop gastric adenocarcinoma, and the lesion stagnated in metaplasia, which corroborates the results obtained by *CDC25B* expression analyses. Based on our hypothesis and previous studies, we suggest *MYC* deregulation is an event that occurs early, during the development of preneoplastic lesions, more specifically in metaplasia.[35] Therefore, MD was not able to prevent the formation of pretumor lesions, but once *MYC* had its expression increased, MD acted to block its effects on *CDC25B* and prevented the progression from metaplasia to adenocarcinoma.

Also, in Figure 6(c.1, d.1, e.1) (atrophic gastritis, metaplasia, intestinal-type adenocarcinoma respectively), the primate was being treated exclusively with MNU, and it is likely that the higher expression of *CDC25B* found in the cytoplasm was caught in the moment of translation, before the protein was transported to the nuclei. This may be due to the high expression and activity of the *CDC25B* gene throughout MNU treatment in *S. apella*, showing a large number of proteins being produced at the cytoplasm. We believe these cells are the ones that are going to evolve to the next steps in gastric carcinogenesis, until they become tumor cells.

On the other hand, in Figure 6(f.1, f.2), the animal was being treated exclusively with MD after the MNU treatment. The inhibition of *CDC25B* expression by MD may reduce protein production at the cytoplasm and, thus, it is not enough to produce cytoplasmic immunoreactivity that is visible under an optical microscope. Therefore, the protein immunoreactivity can only be observed at the nuclei. These findings corroborate our gene expression analysis by RT-qPCR and western blot.

Finally, the animal of the MNU group treated with MD after tumor development demonstrated substantial shrinkage of the tumor. We believe it is due to the decrease of *CDC25B* mRNA and protein expression levels observed at the time of surgical tumor extraction. We suggest this compound had the same action mechanism proposed for the MNU + MD group and ceased tumor progression by inhibiting *CDC25B* expression, thereby inducing cell cycle arrest and stopping tumor cell growth.

A second hypothesis is based on the evidence presented by Sata and colleagues,[36] that MD increases wild-type p53 expression. This transcription factor is known to downregulate *MYC*[37] and *CDC25B* genes.[38,39] Moreover, results from our research group demonstrated that only 7–39% of intestinal-type adenocarcinomas present variations on p53.[40] In this way, MD would be a specific therapy against *MYC* gene amplification, inducing p53 expression which, in turn, decreases the expression of *MYC* and, consequently, of *CDC25B*. However, this hypothesis does not alter our suggestion that MD prevents the consequences of *MYC* deregulation in GC by inhibiting *CDC25B* expression.

## Conclusion

MD was shown to be an effective *CDC25B* inhibitor in GC cell lines, inducing cell cycle arrest and significantly reducing aggressive characteristics of the tumor cells. Our *in-vivo* experiments prove that MD may be an excellent therapeutic strategy,

either in isolation or combined with chemotherapeutics, for patients with GC, especially in more advanced stages, since it was shown to be effective as an antitumor agent in nonhuman primates *S. apella*, reducing tumor size and progression. The *CDC25B* gene was shown to be an attractive therapeutic target in GC and we suggest a clinical trial to evaluate the antitumor potential of MD in patients with advanced gastric tumors as the next step for this study.

### Conflict of interest statement
The authors declare that there is no conflict of interest.

### ORCID iD
Amanda Braga Bona (iD) https://orcid.org/0000-0002-4614-3280

### References
1. Torre LA, Siegel RL, Ward EM, *et al*. Global cancer incidence and mortality rates and trends: an update. *Cancer Epidemiol Biomarkers Prev* 2016; 25: 16–27.

2. Ferlay J, Soerjomataram I, Dikshit R, *et al*. Cancer incidence and mortality worldwide: sources, methods and major patterns in GLOBOCAN 2012. *Int J Cancer* 2015; 136: E359–E386.

3. Da Costa JF, Leal MF, Silva TC, *et al*. Experimental gastric carcinogenesis in *Cebus apella* nonhuman primates. *PLoS One* 2011; 6: e21988.

4. Gutiérrez LG, Delgado MD and León J. *MYC* oncogene contributions to release of cell cycle brakes. *Genes* 2019; 10: 244.

5. De Souza CR, Leal MF, Calcagno DQ, *et al*. *MYC* deregulation in gastric cancer and its clinicopathological implications. *PLoS One* 2013; 8: e64420.

6. Calcagno DQ, Leal MF, Assumpção PP, *et al*. *MYC* and gastric adenocarcinoma carcinogenesis. *World J Gastroenterol* 2008; 14: 5962–5968.

7. Calcagno DQ, Leal MF, Demachki S, *et al*. *MYC* in gastric carcinoma and intestinal metaplasia of young adults. *Cancer Genet Cytogenet* 2010; 202: 63–66.

8. Calcagno DQ, Freitas VM, Leal MF, *et al*. *MYC*, *FBXW7* and *TP53* copy number variation and expression in gastric cancer. *BMC Gastroenterology* 2013; 13: 141.

9. Boutros R, Lobjois V and Ducommun B. CDC25 phosphatases in cancer cells: key players? Good targets? *Nat Rev Cancer* 2007; 7: 495–507.

10. Galaktionov K, Chen X and Beach D. CDC25 cell-cycle phosphatase as a target of c-*myc*. *Nature* 1996; 382: 511–517.

11. Maués JHDS, Ribeiro HF, Pinto GR, *et al*. Gastric cancer cell lines have different *MYC*-regulated expression patterns but share a common core of altered genes. *Can J Gastroenterol Hepatol* 2018; 2018: 1–14.

12. Leal MF, Ribeiro HF, Rey JA, *et al*. YWHAE silencing induces cell proliferation, invasion and migration through the up-regulation of *CDC25B* and *MYC* in gastric cancer cells: new insights about YWHAE role in the tumor development and metastasis process. *Oncotarget* 2016; 7: 85393–85410.

13. Morgan DO. Principles of CDK regulation. *Nature* 1995; 374: 131–134.

14. Nilsson I and Hoffmann I. Cell cycle regulation by the CDC25 phosphatase family. *Prog Cell Cycle Res* 2000; 4: 107–114.

15. Takahashi H, Murai Y, Tsuneyama K, *et al*. High labeling indices of CDC25B is linked to progression of gastric cancers and associated with a poor prognosis. *Appl Immunohistochem Mol Morphol* 2007; 15: 267–272.

16. Li Y, Huang HC, Chen LQ, *et al*. Predictive biomarkers for response of esophageal cancer to chemo(radio)therapy: a systematic review and meta-analysis. *Surg Oncol* 2017; 26: 460–472.

17. Fei F, Qu J, Liu K, *et al*. The subcellular location of cyclin B1 and CDC25 associated with the formation of polyploid giant cancer cells and their clinicopathological significance. *Lab Invest* 2019; 99: 483–498.

18. Ham SW, Park HJ and Lim DH. Studies on menadione as an inhibitor of the CDC25 phosphatase. *Bioorganic Chem* 1997; 25: 33–36.

19. Osada S, Tomita H, Tanaka Y, *et al*. The utility of vitamin K3 (menadione) against pancreatic cancer. *Anticancer Res* 2008; 28: 45–50.

20. Oztopcu-Vatan P, Sayitoglu M, Gunindi M, *et al*. Cytotoxic and apoptotic effects of menadione on rat hepatocellular carcinoma cells. *Cytotechnology* 2015; 67: 1003–1009.

21. Bohla L, Guizzardib S, Rodríguezb V, *et al*. Combined calcitriol and menadione reduces experimental murine triple negative breast tumor. *Biomed Pharmacother* 2017; 94: 21–26.

22. Lee MH, Cho Y, Kim DK, *et al*. Menadione induces G2/M arrest in gastric cancer cells by down-regulation of CDC25C and proteasome mediated degradation of CDK1 and cyclin B1. *Am J Transl Res* 2016; 8: 5246–5255.

23. Leal MF, Nascimento JLM, da Silva CE, *et al*. Establishment and conventional cytogenetic characterization of three gastric cancer cell lines. *Cancer Genet Cytogenet* 2009; 195: 85–91.

24. Leal MF, Calcagno DQ, da Costa Jde FB, *et al*. MYC, TP53, and chromosome 17 copy-number alterations in multiple gastric cancer cell lines and in their parental primary tumors. *J Biomed Biotechnol* 2011; 2011: 631268.

25. Mosmann T. Rapid colorimetric assay for cellular growth and survival: application to proliferation and cytotoxicity. *J Immunol Methods* 1983; 65: 55–63.

26. Russell WMS and Burch RL. *The principles of humane experimental technique*. Wheathampstead: Universities Federation for Animal Welfare, 1959.

27. Kirk RGW. Recovering the principles of humane experimental technique: the 3Rs and the human essence of animal research. *Sci Technol Human Values* 2018; 43: 622–648.

28. Tetef M, Margolin K, Ahn C, *et al*. Mitomycin C and menadione for the treatment of advanced gastrointestinal cancers: a phase II trial. *J Cancer Res Clin Oncol* 1995; 121:103–106.

29. Tetef M, Margolin K, Ahn C, *et al*. Mitomycin C and menadione for the treatment of lung cancer: a phase II trial. *Invest New Drugs* 1995; 13: 157–162.

30. Lauren P. The two histological main types of gastric carcinoma: diffuse and so-called intestinal-type carcinoma. An attempt at a histo-clinical classification. *Acta Pathol Microbiol Scand* 1965; 64: 31–49.

31. Leal MF, Chung J, Calcagno DQ, *et al*. Differential proteomic analysis of noncardia gastric cancer from individuals of Northern Brazil. *PLoS One* 2012; 7: e42255.

32. Livak KJ and Schmittgen TD. Analysis of relative gene expression data using real-time quantitative PCR and the $2^{-\Delta\Delta C_T}$ method. *Methods* 2001; 25: 402–408.

33. Mroczko B, Lukaszewicz-Zajac M, Groblewska M, *et al*. Expression of tissue inhibitors of metalloproteinase 1 (TIMP-1) in gastric cancer tissue. *Folia Histochem Cytobiol* 2009; 47: 511–516.

34. Gong L, Xia Y, Qian Z, *et al*. Overexpression of *MYC* binding protein promotes invasion and migration in gastric cancer. *Oncol Lett* 2018; 15: 5243–5249.

35. Silva TC, Leal MF, Calcagno DQ, *et al. hTERT, MYC* and *TP53* deregulation in gastric preneoplastic lesions. *BMC Gastroenterol* 2012; 12: 85.

36. Sata N, Klonowski-Stumpe H, Han B, *et al*. Menadione induces both necrosis and apoptosis in rat pancreatic acinar AR4-2J cells. *Free Radic Biol Med* 1997; 23: 844–850.

37. Keegan PE, Lunec J and Neal DE. p53 and p53-regulated genes in bladder cancer. *Br J Urol* 1998; 82: 710–720.

38. Ma ZQ, Chua SS, DeMayo FJ, *et al*. Induction of mammary gland hyperplasia in transgenic mice over-expressing human *CDC25B*. *Oncogene* 1999; 18: 4564–4576.

39. Bulavin DV and Fornace AJ Jr. p38 MAP kinase's emerging role as a tumor suppressor. *Adv Cancer Res* 2004; 92: 95–118.

40. Khayat AS, Guimarães AC, Calcagno DQ, *et al*. Interrelationship between TP53 gene deletion, protein expression and chromosome 17 aneusomy in gastric adenocarcinoma. *BMC Gastroenterol* 2009; 9: 55.

Visit SAGE journals online journals.sagepub.com/home/tag

Ⓢ SAGE journals